

# Modeling and Characteristic Analysis of Visco-Hyperelastic Film Based on Biaxial Tensile Experiment

ZHAO Haifeng<sup>1,2</sup>, ZHANG Ya<sup>2\*</sup>, LI Shizhong<sup>2</sup>, LUO Huaan<sup>1</sup>

1. Faculty of Mechanical and Electrical Engineering, Nanjing Vocational College of Information Technology, Nanjing 210023, P.R. China;

2. Faculty of Mechanical and Electrical Engineering, North University of China, Taiyuan 030051, P.R. China

(Received 15 November 2018; revised 18 January 2019; accepted 21 November 2019)

**Abstract:** Dielectric elastomers (DEs) show complex mechanical behaviors with different boundary conditions, geometry sizes, and prestress. In this study, a three-component linear visco-hyperelastic model of DE film is developed based on equibiaxial tension. By applying hereditary integrals to analyze multiple-segment loading processes of film stretching, the model parameters are extracted by fitting the visco-hyperelastic film model to the experimental data. To demonstrate the performance of proposed model, the obtained predictive results are compared with the experimental results under different equibiaxial loading conditions. The good agreement between them shows that the linear visco-hyperelastic model is a promising tool for analytically investigating the property of pre-stretched DE actuators. Finally, the Prony series coefficients are calculated according to the relaxation function. This is helpful for simulation analysis using commercial finite element software.

**Key words:** dielectric elastomers; equibiaxial tension; Prony series; visco-hyperelastic

**CLC number:** TP204      **Document code:** A      **Article ID:** 1005-1120(2019)06-0986-09

## 0 Introduction

Among the deformable electroactive polymers (EAPs), dielectric elastomers (DEs) show impressive expansibility when activated at high voltages, which makes them be used as actuators in adaptive structures<sup>[1-2]</sup>. And DEs have been extensively studied in robots, machine insects, artificial limbs, artificial manipulators and other high-tech research fields in recent years<sup>[3-6]</sup>. Acrylic rubber is an electroactive polymer with viscoelasticity and superelasticity, which is often used as dielectric elastomer actuator. In this study, a visco-hyperelastic film model of an acrylic rubber is evaluated, e.g., VHB4910 from 3M, which has been widely used in DE actuators.

The constitutive model is a mathematical expression reflecting macroscopic properties of materials. It is very important to study the constitutive model of dielectric elastic materials for designing

and optimizing DE actuators. In the early publications about linear elastic materials, the visco-hyperelastic behavior of DEs was seldom involved. The large strain elastic response of elastomer was often modeled by using the strain energy function such as Mooney-Rivlin, Yeoh, and Ogden forms. Simultaneously, the time-dependent functions such as Prony series were used to describe the viscosity<sup>[7-8]</sup>. Hart-Smith reported exponential-hyperbolic elasticity parameters for rubber-like materials over full range of deformations based on the inflation of spherical balloons<sup>[9]</sup> and provided the numerical solutions for the problem of inflation of a circular membrane<sup>[10]</sup>. Guggi Kofod described several elastic models for polymer materials and discussed their discrepancies in different strain ranges<sup>[11]</sup>.

In DE actuators, DE is usually subjected to Maxwell compressive pressure, which is similar to an equibiaxial tensile stress state. Pure shear geome-

\*Corresponding author, E-mail address: zy@nuc.edu.cn.

**How to cite this article:** ZHAO Haifeng, ZHANG Ya, LI Shizhong, et al. Modeling and Characteristic Analysis of Visco-Hyperelastic Film Based on Biaxial Tensile Experiment[J]. Transactions of Nanjing University of Aeronautics and Astronautics, 2019, 36(6):986-994.

<http://dx.doi.org/10.16356/j.1005-1120.2019.06.011>

try<sup>[12-13]</sup> and uniaxially stretched dielectric actuators<sup>[14-20]</sup> are effective methods to evaluate time-dependent behavior and other characteristics of DE actuators. However, the above mentioned methods are not very suitable for the analysis pre-stretched film actuators<sup>[21]</sup>. Zou et al.<sup>[22]</sup> studied hysteresis mechanical model of spring metal-net rubber combination damper. Huang et al.<sup>[23]</sup> reported an anisotropic visco-hyperelastic constitution model for cord-rubber. Tan et al.<sup>[24]</sup> proposed a transversely isotropic visco-hyperelastic constitutive model for short fiber reinforced EPDM. Wang<sup>[25]</sup> studied the visco-elastic behavior of a circular dielectric elastomer film actuator under electromechanical coupling. Chen et al.<sup>[26]</sup> discussed a hyperelastic constitutive model for membrane and its application in air cushion. David et al.<sup>[27]</sup> presented the governing equations for the electromechanically coupled behavior of dielectric elastomers in a thermodynamic framework and discussed the attendant finite-element formulation and implementation by using a commercial finite-element code. Although many hyperelastic constitutive models describing polymers have been proposed by researchers at home and abroad, little research has been done on the visco-hyperelastic deformation of acrylate rubber.

In this study, a visco-hyperelastic model of dielectric elastomer acrylic rubber film is proposed based on an equibiaxial tensile experiment. By applying hereditary integrals to analyze multiple-segment loading processes of film stretching, the model parameters are extracted by fitting the visco-hyperelastic film model to the experimental data. The mechanical response of visco-hyperelastic film is expressed using a three-component model. Then hereditary integrals are applied to analyze multiple-segment loading experiment, and the model parameters are extracted by fitting with the equibiaxial experimental data. The mechanical responses under different loadings are also predicted and compared with the experimental data. The Prony series coefficients are calculated using the model parameters. And some conclusions of this study are provided. The linear visco-hyperelastic model can be used to evaluate the property of equibiaxially pre-stretched

DE actuators.

## 1 Visco-Hyperelastic Model for Square Film

First, the proposed model does not provide a general description of visco-hyperelastic polymers. It can serve as a tool to analyze the characteristics of DE actuators. Because Maxwell and Voigt models describe only the relaxation and creep characteristics, respectively<sup>[21]</sup>, the multi-component model is used to describe the actual visco-hyperelastic model, which should be nondegenerate.

Basically, it is helpful to assume that the model of film is composed of countless microcubes with the same cross-sectional area and the length, as shown in Fig.1(a). Each segment of the cube consists of two springs and one dashpot, as shown in Fig.1(b).

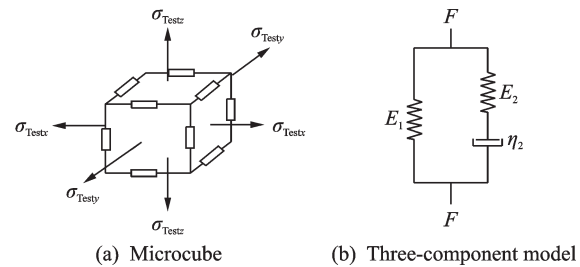


Fig.1 Schematic of linear visco-hyperelastic model

To simplify the analysis, the following conditions are required for the model.

- (1) Visco-hyperelastic material is an isotropic and homogeneous medium.
- (2) The central zone of film in the equibiaxial tensile experiment is uniformly subjected to contraction or elongation deformation, i.e., by neglecting the shear effect.
- (3) Visco-hyperelastic film is incompressible.

Other assumptions such as mass-free, cuboid geometry maintained under deformation<sup>[14]</sup> are also required.

In this study, as is shown in Fig.1(b), a three-component model is used, in which a spring is linked with a dashpot and two components are linked with another spring in parallel (i.e., the Kelvin model). Here  $E_1$  and  $E_2$  are the stiffnesses which

are defined by  $k_i/s^{(0)}$ ,  $i=1,2$ , where  $s^{(0)}$  is the original length of segment and  $k_i$  is the stiffness coefficient of spring in Fig.1(b). And  $\eta_2$  is damping coefficient which is defined by  $d/s^{(0)}$ , where  $d$  is the damping coefficient of dashpot. As the approximation, it is assumed that the cube consisting of a spring-dashpot is filled with incompressible fluid, and the hydrostatic pressure varies with the deformation of the cube.  $E_1$ ,  $E_2$ , and  $\eta_2$  in the spring-dashpot system are also assumed to be constant, and  $\sigma_{Testi}$  ( $i=x, y$  and  $z$ ) are external normal stress of the cube.

In the above mentioned model, the spring is the linear-elastic component, and the dashpot is the viscous component. In the model, the stress of each component is equal, and the total strain is the sum of individual strains in series connection. The total stress is the sum of stress in each link, and the strain in each link is equal in the parallel connection. As shown in Fig. 1 (b), when the external force  $F(t)$  is applied, the force equilibrium results in a differential equation for the deformation behavior in three directions, which is

$$\frac{dS}{dt} + \frac{E_2}{\eta_2} S = (E_1 + E_2) \frac{d\epsilon}{dt} + \frac{E_1 E_2}{\eta_2} \epsilon \quad (1)$$

where the stress is defined by  $S = F/(s^{(0)})^2$ .  $F$  is the external force,  $d\epsilon/dt$  the deformation rate, and  $\epsilon$  the strain. When the step strain  $\epsilon(t) = \epsilon_0 H(t)$  is applied to the model, the relaxation stress formula can be obtained by solving Eq.(1).

$$S(t) = E_1 \epsilon_0 + E_2 \epsilon_0 \exp\left(-\frac{t}{t_{b2}}\right) \quad (2)$$

where  $t_{b2} = \eta_2/E_2$  is the retardation time. Therefore, the relaxation function  $E(t)$  can be expressed as

$$E(t) = E_1 + E_2 \exp\left(-\frac{t}{t_{b2}}\right) \quad (3)$$

When equibiaxially stretched, the film is extended in the  $x, y$  directions and contracted in the  $z$  direction. The external normal stress of  $\sigma_{Testi}$  ( $i=x, y$ , and  $z$ ) can be expressed by

$$\begin{cases} \sigma_{Testx} = \sigma_{Testy} = \sigma_{Test} \\ \sigma_{Testz} = 0 \end{cases} \quad (4)$$

During the deformation, the internal hydrostatic pressure  $p(t)$  diverges from zero. The force equilibrium

across the wall of deformed cuboid results in<sup>[12]</sup>

$$\sigma_{Testi} = \lambda_i S_i - p \quad i=x, y, z \quad (5)$$

where  $\lambda_i$  are the stretch ratios. The stretch ratios  $\lambda_i = s_i/s_i^{(0)}$  are the ratios of the deformed dimension to the original dimension of the film.

## 2 Equibiaxial Tensile Experimental Analysis

The parameters of the visco-hyperelastic model can be derived from the experimental data, and then the performance of the dielectric actuator can be analyzed. The experiments include creep, relaxation, constant rate stress, constant rate strain and dynamic measurement<sup>[28]</sup>.

In this study, the visco-hyperelastic model is analyzed by designing an equibiaxial tensile experiment apparatus. The working principle of the equibiaxial tensile experiment is shown in Fig. 2. Two stepping motors (not shown in the Fig. 2.) drive two pairs of reverse screw rods to rotate. Thus, two pairs of slideways of  $X$  and  $Y$  axes are driven to move equibiaxially symmetrically along  $X$  and  $Y$  directions respectively. The specimens are clamped by 20 self-tightening clamps with uniform distribution around them. In the center of specimen, four dark orthogonal markers are printed for measuring the displacement. The experimental specimens are in the form of square sheets, which are 9 cm long on each side and 1 mm thick. Two load cells are mounted on the two sides of slideway. While stretching symmetrically, the bearings on the back of self-tightening collets slide along the slideway al-

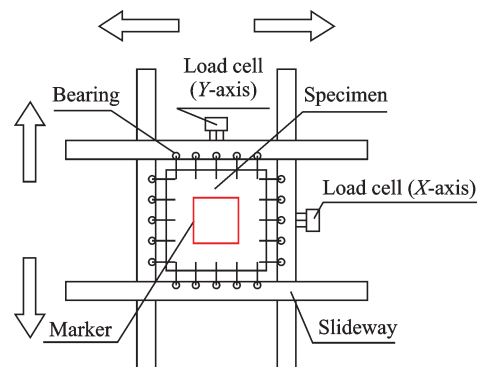


Fig.2 Principle of equibiaxial tension experiment

most simultaneously. The strain of the sample can be measured by the caliper and the tension can be collected by force sensor. Fig.3 is the design of the equibiaxial tension experiment apparatus.

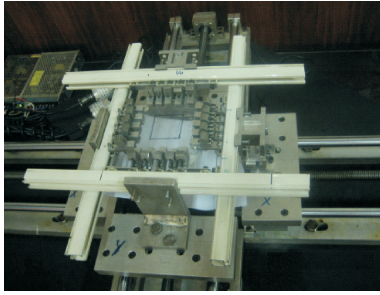


Fig.3 Equibiaxial tension experiment apparatus

### 2.1 Multiple-segment loading process

In the tension, the ideal creep and relaxation experiments cannot be satisfied, so the model parameters are obtained by multiple-segment loading on the biaxial experiment apparatus at approximately constant tension rate<sup>[29-30]</sup>.

Under equibiaxial tension condition, according to the incompressibility ( $\lambda_x \lambda_y \lambda_z = 1$ ), the following equations can be formulated.

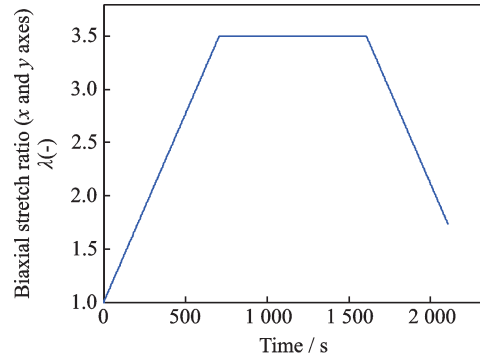
$$\begin{aligned} \lambda_x &= \lambda_y = \lambda = 1 + \epsilon(t) \\ \lambda_z &= 1/\lambda^2 \end{aligned} \quad (6)$$

It is observed that the deformation in  $z$ -axis direction is different from that in  $x$  and  $y$  axes directions. The equibiaxial multiple-segment loading processes are shown in Fig.4, which can be divided into three segments. Firstly, the film samples are equibiaxial stretched at a tensile rate of  $3.54e-3$ , then maintained 900 s, and finally regressed at the same rate.

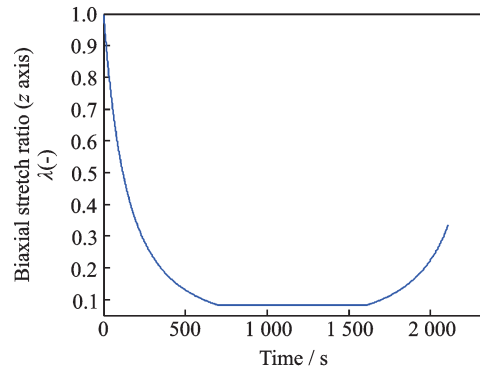
The strain rate functions in  $x$ ,  $y$  axes directions are defined as

$$\frac{d\epsilon_x}{dt} = \frac{d\epsilon_y}{dt} = \frac{d\epsilon}{dt} = \frac{d\lambda}{dt} = \begin{cases} \epsilon_1/t_1 & 0 < t \leq t_1 \\ 0 & t_1 < t \leq t_2 \\ -\epsilon_1/(t_3 - t_2) & t_2 < t \leq t_3 \end{cases} \quad (7)$$

Owing to the incompressibility, the straining rate in  $z$  axis is not constant. To facilitate the subsequent analysis, the stretch ratio in  $z$  axis can be expressed with 4th degree polynomial in  $\lambda$  in the first and third segments. According to the defined stretch



(a)  $\lambda$  of  $x$  and  $y$  axes



(b)  $\lambda$  of  $z$  axis

Fig.4 Equibiaxial multiple-segment loading processes

ratio of equibiaxial tensile experiment, where the stretch ratio is  $\lambda = 3.5$ , the polynomial can be fitted with Matlab (see Eq.(8), the fitting range is up to  $\lambda = 4$ ). Then the strain rate in  $z$ -axis direction can be obtained by differentiating the stretch ratio  $\lambda_z$  with respect to time  $t$  (see Eq.(9)).

$$\lambda_z = \frac{1}{\lambda^2} = 0.04947\lambda^4 - 0.5837\lambda^3 + 2.572\lambda^2 - 5.106\lambda + 4.041 \quad (8)$$

$$\frac{d\epsilon_z}{dt} = \frac{d\lambda_z}{dt} = (0.19788\lambda^3 - 1.7511\lambda^2 + 5.144\lambda - 5.106) \frac{d\epsilon}{dt} \quad (9)$$

Substituting Eqs.(6, 7) into Eq.(9), different strain rates of three segments in  $z$ -axis direction can be obtained.

### 2.2 Application of hereditary integrals to multiple loading process

To determine the stress in a visco-hyperelastic material at a given time, the deformation history should be considered. For a linear visco-hyperelastic material, a superposition of hereditary integrals can be used to describe the time-dependent response. According to the relaxation function, the stress

equation in the film model can be expressed as

$$S(t) = \varepsilon_0 E(t) + \int_0^t E(t-\xi) \frac{d\varepsilon(\xi)}{d\xi} d\xi \quad (10)$$

In equibiaxial multiple-segment loading processes, with  $\varepsilon_0 = \varepsilon(0) = 0$ , the stress functions in each segment can be shown as follows.

**Step 1** By equibiaxially stretching the square film ( $0 < t \leq t_1$ ), the stress response depends on the imposed constant-rate straining as

$$S_x^I(t) = S_y^I(t) = \int_0^t E(t-\xi) \frac{d\varepsilon_x^I(\xi)}{d\xi} d\xi \quad (11)$$

$$S_z^I(t) = \int_0^t E(t-\xi) \frac{d\varepsilon_z^I(\xi)}{d\xi} d\xi \quad (12)$$

where index I represents Step 1. Note that under the deformation, the internal hydrostatic pressure of  $p(t)$  changes simultaneously. Therefore,

$$\sigma_{\text{Test}x}^I(t) = \sigma_{\text{Test}y}^I(t) = \lambda_x^I(t) S_x^I(t) - p^I(t) \quad (13)$$

$$\sigma_{\text{Test}z}^I(t) = \lambda_z^I(t) S_z^I(t) - p^I(t) = 0 \quad (14)$$

Solving Eqs. (11–14) and substituting  $\lambda_z^I = (\lambda^I)^{-2}$  into the results yield

$$\sigma_{\text{Test}x}^I(t) = S_x^I(t) \left(1 + \frac{\varepsilon_1}{t_1} t\right) - S_z^I(t) \left(1 + \frac{\varepsilon_1}{t_1} t\right)^{-2} \quad (15)$$

**Step 2** Relaxation ( $t_1 < t \leq t_2$ ). Using the first and second strain ingrates yields

$$S_x^{\text{II}}(t) = \varepsilon_0 E(t) + \int_0^{t_1} E(t-\xi) \frac{d\varepsilon_x^I(\xi)}{d\xi} d\xi + \int_{t_1}^t E(t-\xi) \frac{d\varepsilon_x^{\text{II}}(\xi)}{d\xi} d\xi = \quad (16)$$

$$\int_0^{t_1} E(t-\xi) \frac{d\varepsilon_x^I(\xi)}{d\xi} d\xi$$

$$S_z^{\text{II}}(t) = \varepsilon_0 E(t) + \int_0^{t_1} E(t-\xi) \frac{d\varepsilon_z^I(\xi)}{d\xi} d\xi + \int_{t_1}^t E(t-\xi) \frac{d\varepsilon_z^{\text{II}}(\xi)}{d\xi} d\xi = \quad (17)$$

$$\int_0^{t_1} E(t-\xi) \frac{d\varepsilon_z^I(\xi)}{d\xi} d\xi$$

where index II represents step2. Considering the internal hydrostatic pressure of  $p(t)$ , the tensile stress can be derived as

$$\sigma_{\text{Test}x}^{\text{II}}(t) = S_x^{\text{II}}(t)(1 + \varepsilon_1) - S_z^{\text{II}}(t)(1 + \varepsilon_1)^{-2} \quad (18)$$

**Step 3** Regression ( $t_2 < t \leq t_3$ ). The stress responses to the imposed constant-rate straining  $-\varepsilon_1/(t_3 - t_2)$  are as follows.

$$S_x^{\text{III}}(t) = \varepsilon_0 E(t) + \int_0^{t_1} E(t-\xi) \frac{d\varepsilon_x^I(\xi)}{d\xi} d\xi + \int_{t_1}^{t_2} E(t-\xi) \frac{d\varepsilon_x^{\text{II}}(\xi)}{d\xi} d\xi + \int_{t_2}^t E(t-\xi) \frac{d\varepsilon_x^{\text{III}}(\xi)}{d\xi} d\xi = \quad (19)$$

$$S_x^{\text{II}}(t) + \int_{t_2}^t E(t-\xi) \frac{d\varepsilon_x^{\text{III}}(\xi)}{d\xi} d\xi$$

$$S_z^{\text{III}}(t) = S_z^{\text{II}}(t) + \int_{t_2}^t E(t-\xi) \frac{d\varepsilon_z^{\text{III}}(\xi)}{d\xi} d\xi \quad (20)$$

$$\sigma_{\text{Test}x}^{\text{III}}(t) = S_x^{\text{III}}(t) \lambda_x^{\text{III}}(t) - S_z^{\text{III}}(t) \lambda_z^{\text{III}}(t) =$$

$$S_x^{\text{III}}(t) \left( \varepsilon_1 - \frac{\varepsilon_1}{t_3 - t_2} t + 1 \right) - \quad (21)$$

$$S_z^{\text{III}}(t) \left( \varepsilon_1 - \frac{\varepsilon_1}{t_3 - t_2} t + 1 \right)^{-2}$$

where index III represents step 3.

### 2.3 Fitting of visco-hyperelastic film model

The VHB4910 double-sided adhesive manufactured by 3M Company has been tested by multiple-segment tensile experiment on equibiaxial tension apparatus. The experimental data are shown in Fig.5(a). By fitting Eqs.(15, 18, 21) to the experimental data, the model parameters ( $E_1$ ,  $E_2$  and  $\eta_2$ ) can be obtained. To optimize the parameters, another equibiaxial tension experiment is applied to the same specimen, whose experimental data are shown in Fig.5(b). By fitting and synthesizing the two experimental results, the final parameters are as follows:  $E_1 = 0.021 \text{ N}\cdot\text{mm}^{-2}$ ,  $E_2 = 0.017 \text{ N}\cdot\text{mm}^{-2}$ , and  $\eta_2 = 1.75 \text{ N}\cdot\text{s}\cdot\text{mm}^{-2}$ .

The two experimental specifications are shown in Table 1.

Experiment 1 shows that the predicted model agrees well with the experimental data when the tension rate and relaxation rate are the same. Experiment 2 shows that experimental data are also in good agreement with the fitting model when the tensile ratio and regression ratio are quite different.

After obtaining the visco-hyperelastic model parameters, the different stress response curves at different stretch rates and stretch ratios can be predicted. The predicted stress response curves at different stretch rates are shown in Fig.6 when  $\lambda = 3.5$ . The predicted stress response curves at different stretch

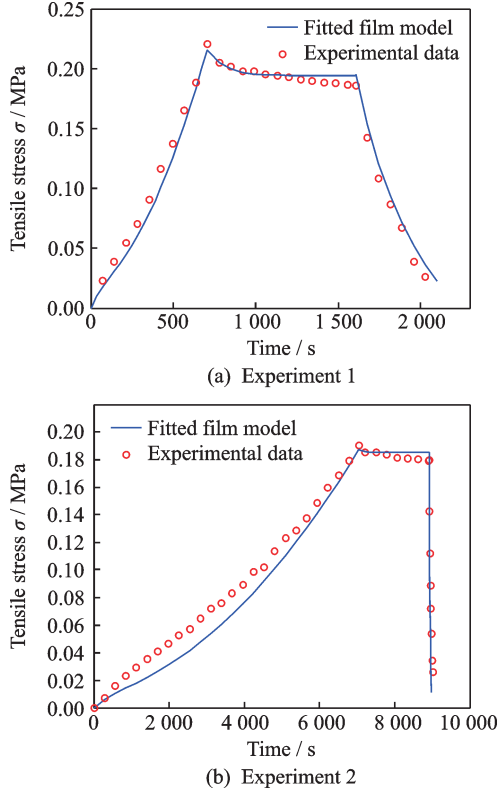


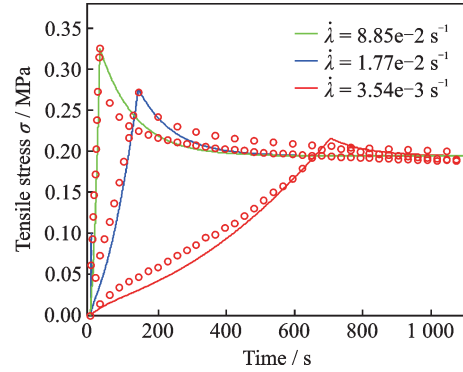
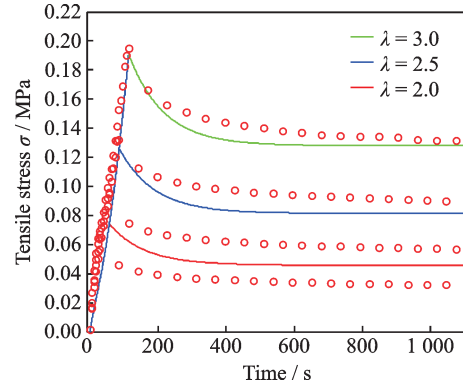
Fig.5 Fitting of visco-hyperelastic film model

**Table 1 Experimental specification**

Experiments	Stretch rate	Relaxation	Regress rate
	$\dot{\lambda}/s^{-1}$	time/s	$\dot{\lambda}/s^{-1}$
Experiment 1	$3.54e-3$	900	$3.54e-3$
Experiment 2	$3.54e-4$	1 820	$1.76e-2$

ratios are shown in Fig. 7 when  $\dot{\lambda}=1.77e-2 s^{-1}$ . The predicted results show that the tensile rate affects the maximum response stress, and the tensile ratio determines the quasi-static stress. Simultaneously, the predicted results (fitted film model (—)) are compared with the experimental data (○), and the results show that both agree well within the experimental range. The deviation is observed when the stretch ratios are low (either during stretching or relaxation). The error is related to the accuracy of the experiment itself. In addition, the tensile-relaxation experiment is carried out by means of square uniform point clamping method. The film deformation at clamping position and non-clamping position is not uniform. In the case of small tensile ratio, the non-linear characteristics of deformation are particularly prominent, which results in the deviation of ex-

perimental stress from the fitting ones. Eliminating above factors, the fitting stress curve of the film is basically consistent with the experimental data, and the trend and smoothness of the curve are very similar, which shows that the visco-hyperelastic model is effective.

Fig.6 Stress response curves at different stretch rates when  $\lambda=3.5$ Fig.7 Stress response curves at different stretch ratios when  $\dot{\lambda}=1.77e-2 s^{-1}$ 

### 3 Deduction of Prony Series Coefficients

The visco-hyperelastic model based on strain energy is an effective method for describing the quasi-linear visco-hyperelastic of materials. In most finite element packages, the linear visco-hyperelastic model is specified by a relaxation function of Prony series. The visco-hyperelastic material parameter  $C_{ij}^R$  in strain energy potential can be expressed as<sup>[7]</sup>

$$C_{ij}^R(t) = C_{ij}^0 \left[ 1 - \sum_{k=1}^N g_k \left( 1 - \exp\left(-\frac{t}{t_k}\right) \right) \right] \quad (22)$$

where  $C_{ij}^0$  is the instantaneous elastic response, and  $g_k$  and  $t_k$  characterize the relaxation behavior.

Generally, the assumption of quasi-linear visco-elasticity is that the stress relaxation function is independent of the magnitude of deformation. This can be verified by equibiaxial relaxation experiment under different stretch ratios. Fast manual experiments are performed on a biaxial experiment apparatus by equibiaxially stretching the square films quickly (0.2—0.5 s) to a predefined elongation ( $\lambda=2.5, 2, 1.5$ ), then fixing the sample with a special fixture to relax. The relaxation force is sampled from the force sensor along  $X$  and  $Y$  axes, and the average values of  $X$  and  $Y$  axes data are obtained (Fig. 8). The nominal stress  $S$  after long relaxation (1 500 s) is normalized.

It can be seen from Fig.9 that several normalized relaxation curves are very close to each other, which can verify the quasi-linear hypothesis.

Means of normalized experimental curves are also used to compare with other analytical results (see Fig.10).

Based on the relaxation function shown in Eq.(3), the Prony series coefficients can be calculated. Under equibiaxial relaxation condition, by normalizing relaxation stress  $S(t)$  (i.e., Eq.(2)) and Prony series, the following formulations can be deduced.

$$S_{\infty}(t) = \frac{S(t)}{S(\infty)} = 1 + \frac{E_2}{E_1} \exp\left(-\frac{t}{t_{b2}}\right) \quad (23)$$

$$S_{\text{Prony}} = \frac{1 - \sum_{k=1}^N g_k \cdot \left(1 - \exp\left(-\frac{t}{t_k}\right)\right)}{1 - \sum_{k=1}^N g_k} \quad (24)$$

Comparing Eq.(23) with Eq.(24), one-term Prony series coefficients can be obtained. By solving

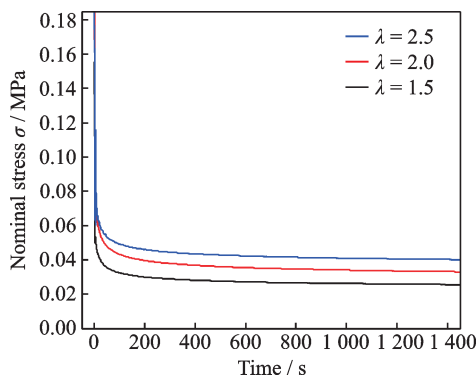


Fig.8 Nominal stress versus time at different elongations

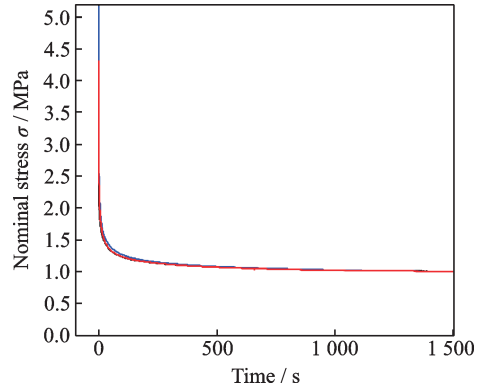


Fig.9 Normalized nominal stress from different experiments

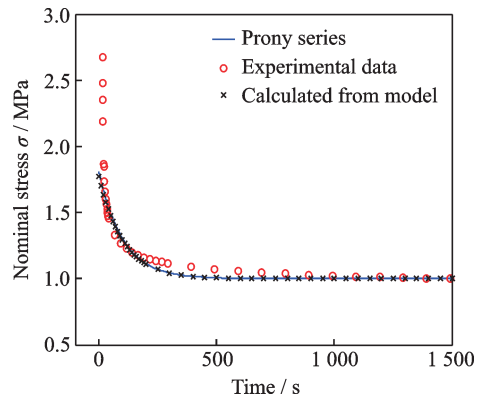


Fig.10 Comparison of different normalized stress and Prony series

Eq.(25), the final results are as follows:  $g_1=0.447$ ,  $t_1=102.9$ . Fig. 10 shows a comparison of different normalized stress and Prony series. The deviation occurs at the beginning of relaxation period. The reasons lie in: (1) When rapidly stretching the film, the viscous effect is significant and thus the stress is tremendous; (2) There is a gap between the ideal step deformation and the manual rapid tension rate, so the initial stress value cannot be given accurately. It can be concluded that the visco-hyperelastic model mentioned above is adequate for quasi-static analysis.

$$\begin{cases} \frac{E_2}{E_1} = \frac{g_1}{1 - g_1} \\ t_1 = \frac{\eta_2}{E_2} \end{cases} \quad (25)$$

### 4 Conclusions

A three-component visco-hyperelastic model can be used to describe the time-dependent mechanical response of a visco-hyperelastic film under equibi-

axial tensile condition. The model parameters can be extracted through equibiaxial multiple loading experiments. The relationship between model parameters and one-term Prony series can be deduced through the normalization. The results show that the analysis and experiment agree well, providing the evidence for the evaluation of subsequent equibiaxially pre-stretched DE actuators. Finally, when using linear visco-hyperelastic model in practical application, appropriate working conditions and stretching range should be considered. The effect of tensile ratio on model parameters needs further study.

### References

- [1] PELRINE R, KORNBLUH R, PEI Q B, et al. High-speed electrically actuated elastomers with strain greater than 100% [J]. *Science New Series*, 2000, 287 (5454):836-839.
- [2] PELRINE R, KORNBLUH R, KOFOD G. High-strain actuator materials based on dielectric elastomers [J]. *Advanced Materials*, 2000, 12 (16):1223-1225.
- [3] SON S, GOULBOURBNE N C. Finite deformations of tubular dielectric elastomer sensors [J]. *Journal of Intelligent Material Systems and Structures*, 2009, 20 (18):2187-2199.
- [4] CARPI F, FREDIANI G, DE ROSSI D. Hydrostatically coupled dielectric elastomer actuators [J]. *IEEE/ASME Transactions on Mechatronics*, 2010, 15(2): 308-315.
- [5] LIU K, CHEN Y N, WU Y, et al. Rotation control of a 3-DOF parallel mechanism driven by pneumatic muscle actuators [J]. *Transactions of Nanjing University of Aeronautics and Astronautics*, 2019, 36(2): 330-338.
- [6] LUO H A, WANG H M, YOU Y P. Analysis of electromechanical coupling activation process of dielectric elastomer cylindrical actuator [J]. *Journal of Nanjing University of Aeronautics and Astronautics*, 2012, 44(6): 869-875. (in Chinese)
- [7] FUNG Y C. Biomechanics: Mechanical properties of living tissues [J]. *The Quarterly Review of Biology*, 1994, 69(4): 568-569.
- [8] WISSLER M, MAZZA. Modeling of a pre-strained circular actuator made of dielectric elastomers [J]. *Sensors and Actuators A: Physical*, 2005, 120(1): 184-192.
- [9] HART-SMITH L. J. Elasticity parameters for finite deformations of rubber-like materials [J]. *Zeitschrift für Angewandte Mathematik und Physik (ZAMP)*, 1967, 17(5):608-626.
- [10] HART-SMITH L J, CRISP J D C. Large elastic deformations of thin rubber membranes [J]. *International Journal of Engineering Science*, 1967, 5(1): 1-24.
- [11] KOFOD G. Dielectric elastomer actuators [D]. Roskilde: Technical University of Denmark, 2001.
- [12] KOFOD G, SOMMER-LARSEN P. Silicone dielectric elastomer actuators: Finite-elasticity model of actuation [J]. *Sensors and Actuators A: Physical*, 2005, 122(2):273-283.
- [13] TANG X F. Response analysis of quartz crystal resonator and its application in studies of viscoelastic thin films [D]. Hefei: University of Science and Technology of China, 2014. (in Chinese)
- [14] LOCHMATTER P, KOVACS G, MICHEL S. Characterization of dielectric elastomer actuators based on a hyperelastic film model [J]. *Smart Materials and Structures*, 2007, 16(2):748-757.
- [15] PATRICK L, KOVACS G, WISSLER M. Characterization of dielectric elastomer actuators based on a visco-hyperelastic film model [J]. *Smart Materials and Structures*, 2007, 16(1): 477-486.
- [16] GALLIOT C, LUCHSINGER R H. Uniaxial and biaxial mechanical properties of ETFE foils [J]. *Polymer Testing*, 2011, 30(4):356-365.
- [17] BRIDGENS B N, GOSLING P D. Interpretation of results from the MSAJ testing method for elastic constants of membrane materials [J]. *Neuroscience Letters*, 2010, 612: 14-17.
- [18] MBROZIAK A, KLOSOWSKI P. Mechanical properties for preliminary design of structures made from PVC coated [J]. *Fabric Construction Building Materials*, 2014, 50: 74-81.
- [19] MOSTAFA N H, ISMARRUBIE Z N, SAPUAN S M, et al. Effect of fabric biaxial prestress on the fatigue of woven E-glass / polyester composites [J]. *Materials & Design*, 2016, 92: 579-589.
- [20] AMBROZIAK A. Mechanical properties of Precontrain1202S coated fabric under biaxial tensile test with different load ratios [J]. *Construction & Building Materials*, 2015, 80: 210-224.
- [21] SASSO M, PALMIERI G, CHIAPPINI G, et al. Characterization of hyperelastic rubber-like materials by biaxial and uniaxial stretching tests based on optical methods [J]. *Polymer Testing*, 2008, 27(8): 995-

- 1004.
- [22] ZOU G P, ZHANG B, CHANG Z L. Hysteresis mechanical model and experimental study of spring metal-net rubber combination damper [J]. Chinese Journal of Theoretical and Applied Mechanics, 2018, 50 (5) : 1125-1134. (in Chinese)
- [23] HUANG X S, PENG X Q, ZHANG B C. An anisotropic visco-hyperelastic constitutive model for cord-rubber composites [J]. Chinese Journal of Theoretical and Applied Mechanics, 2016, 48(1) : 140-145. (in Chinese)
- [24] TAN B D, XU J S, SUN C X, et al. A transversely isotropic visco - hyperelastic constitutive model for short fiber reinforced EPDM[J]. Chinese Journal of Theoretical and Applied Mechanics, 2017, 49 (3) : 677-684. (in Chinese)
- [25] WANG B. Investigation on the viscoelastic behaviors of dielectric elastomer membrane actuators[D]. Lanzhou: Lanzhou University of Technology, 2017. (in Chinese)
- [26] CHEN M, PENG X Q, SHI S Q, et al. A hyperelastic constitutive model for membrane and its application in air cushion [J]. Journal of Shanghai Jiao Tong University , 2014, 48(6):883-887. (in Chinese)
- [27] DAVID L H, SHAWN A C, KATIA B. Modeling of dielectric elastomers: Design of actuators and energy harvesting devices[J]. Journal of the Mechanics and Physics of Solids, 2013 ,61(10): 2047-2066.
- [28] ZHANG S S, ZHUANG Z. Composites and viscoelastic mechanics[M]. Beijing: Machinery Industry Press, 2011: 52-67. (in Chinese)
- [29] LUO H A, WANG H M , YOU Y P. Experimental methods of equiaxial tension of hyperelastic membrane and corresponding simulations[J]. Journal of South China University of Technology, 2011, 39(4) : 56-61. (in Chinese)
- [30] LUO H A. Research on characteristics of cylindrical dielectric electroactive polymer actuator [D]. Nanjing: Nanjing University of Aeronautics and Astronautics, 2015. (in Chinese)

**Acknowledgements** This work was supported by the Natural Science Fund for colleges and universities in Jiangsu Province (No. 18KJB530012), Advanced Study of Professional

Leaders in Higher Vocational College of Jiangsu Province (No.2019GRGDYX113), National Key Research and Development Program (No.2017YFB1300600), the Middle-aged & Young key teachers of Colleges and Universities of Jiangsu Province (Grant:2016-15), and PhD Foundation of Nanjing Institute of Information Technology (No.YB20160201).

**Authors** Mr. ZHAO Haifeng received his B.S. degree in Mechanical Design and Automation and M.S. degree in Precision Instrument and Machinery from North University of China in 2004 and 2009, respectively. Now he is a Ph.D. candidate and an associate professor. His research has focused on sensor design, target information detection and recognition technology and smart materials and their applications.

Prof. ZHANG Ya received his B.S. degree in Precision Electromechanical Device from Taiyuan Institute of Machinery in 1984 and Ph.D. degree in Mechanics and Robot Technology from National Moscow University of Technology in 1995. His research has focused on the design and analysis of mechanical and electrical systems, the control technology of mechanical and electrical systems, and the detection and recognition technology of targets and environment.

Prof. LI Shizhong received his B.S. degree in Electronic Precision Machinery from Taiyuan Institute of Machinery in 1991 and Ph.D. degree in Mechanical and Electronic Engineering from Beijing Institute of Technology in 2004. His research has focused on target detection and recognition technology, information processing and control technology.

Dr. LUO Huaan received his M. S. degree in Mechanical Manufacturing and Automation from Xi'an University of Science and Technology in 2005, and Ph.D. degree in Mechanical and Electronics Engineering from Nanjing University of Aeronautics and Astronautics in 2015. His research interests include smart materials and their applications.

**Author contributions** Mr. ZHAO Haifeng completed the experiments, conducted the analysis and wrote the manuscript. Prof. ZHANG Ya and Prof. LI Shizhong contributed to the discussion and background for the study. Dr. LUO Huaan designed the study and guided the experiments.

**Competing interests** The authors declare no competing interests.

(Production Editor: Wang Jing)